GSA Data Repository 2018074
Richter et al., 2018. Hydrothermal formation of heavy rare earth element (HREE)–xenotime deposits at 100 °C in a sedimentary basin: Geology, https://doi.org/10.1130/G39871.1.

Details of Analytical Methods, Sample Locations and Fluid Inclusion Analyses

Microthermometric measurements were performed at GFZ Potsdam and TU Bergakademie Freiberg on 51 quartz-hosted fluid inclusions from well-defined assemblages (i.e. groups of inclusions that are unequivocally coeval based on petrographic relations; see Diamond, 1990; Goldstein and Reynolds, 1994) from 5 sample locations (Tables A1 and A2). A fully automated Linkam THSG 600 heating-freezing stage was used, mounted on an Olympus BX 51 (GFZ Potsdam)/ BX 53 (TU Bergakademie Freiberg) microscope. The Linkam stage was calibrated with synthetic fluid inclusions. Salinities of the studied fluid inclusions were calculated from the temperature at which the last crystal of ice melts in the presence of vapor upon gradual heating, T_m(Ice), using the calibration of Steele-MacInnis et al. (2012) for the model H_2O–NaCl system. Homogenization temperatures, T_h, were measured by observing bubble-point transitions (LV→L). As the inclusions were trapped in the heterogeneous state (i.e. from coexisting liquid + vapor, see text), the lowest of the recorded T_h values are equivalent to the fluid trapping temperature (see Diamond, 2003, for principles).

Laser Raman analyses were conducted on confocal Jobin Yvon Horiba instruments at GFZ Potsdam (Triple LABRAM) and University of Bern (LABRAM HR-800) using a 532 nm laser.

Cathodoluminescence (CL) measurements were done on carbon-coated, polished thin sections using a “hot cathode” CL microscope HC1-LM (Neuser et al. 1995) at the TU Bergakademie Freiberg. The system was operated at 14 kV accelerating voltage and a current of 0.2 mA (current density of ~10 µA/mm^2). Luminescence images were captured "on-line" during CL irradiation using a peltier-cooled, digital video-camera (OLYMPUS DP72).

Liquid-rich L+V inclusions from primary assemblages in quartz-2 were selected for LA-ICP-MS analysis (Tables A3 and A4) at the University of Leeds using an ArF 193 nm Geolas Q Plus excimer laser equipped with imaging optics. Analyses were performed with an Agilent 7500c quadrupole ICP-MS equipped with an octopole reaction cell. In this study, several inclusions from a given assemblage were analyzed for the cations Na, Mg, K, Ca, Fe, Cu, Zn, Y, Pb, U, and the remaining inclusions in the same assemblage were analyzed for Na and REE The analyses were calibrated against NIST standards SRM 610 and the acquired signals were processed using the software package "Sills" developed at the ETH Zurich by Guillong et al. (2008). The apparent limit of detection for phosphorous is based on the mass-31 signal in the host quartz and it is around 40% of the Na concentration. However, this value is massively elevated by the presence of ^{16}O-^{15}N ion pairs in the plasma, as often observed in La-ICP-MS analysis of P in silicate minerals (Lehmann et al., 2011). The element ratios were recast as concentrations based on the 25 wt.-% $NaCl_{eq}$ salinity by lumping monovalent KCl with NaCl, and bivalent $MgCl_2$ and $FeCl_2$ with $CaCl_2$, to model the measured T_m(ice) values within the ternary H_2O–NaCl–$CaCl_2$ system using experimental data in Oakes et al. (1990) .

References

Cook, N.J.. Ciobanu, C.L, O'Reilly, D., Wilson, R., Das, K., and Wade, B., 2013, Mineral chemistry of rare earth element (REE) mineralization, Browns Range, Western Australia: Lithos, v. 172–173, p. 192–213.

Diamond, L.W., 1990, Fluid inclusion evidence for P-V-T-X evolution of hydrothermal solutions in Late-Alpine gold-quartz veins at Brusson, Val d'Ayas, NW Italian Alps, American Journal of Science, v. 290, p. 912–958.

Diamond, L.W., 2003, Systematics of H_2O inclusions, in Samson, I.M., Anderson, A.J., and Marshall, D.D., eds., Short Course 32. Fluid Inclusions: Analysis and Interpretation, Mineralogical Association of Canada, p. 55–79.

Goldstein, R.H., and Reynolds, T.J., 1994, Systematics of fluid inclusions in diagenetic

minerals, Tulsa, Society for Sedimentary Geology, SEM Short Course.

Guillong M., Meier D.L., Allan M.M., Heinrich C.A., and Yardley B.W.D., 2008, SILLS: A MATLAB-based program for the reduction of laser ablation ICP-MS data of homogeneous materials and inclusions. In Laser ablation ICP-MS in the Earth sciences: Current practices and outstanding issues, edited by Sylvester P., Mineralogical Association of Canada, Short Course 40, p. 328–333.

Lehmann, K, Pettke, T and Ramseyer, K. 2011, Significance of trace elements in syntaxial quartz cement, Haushi Group sandstones, Sultanate of Oman, Chemical Geology, 280, p. 47-57.

Neuser, R.D., Bruhn, F., Götze, J., Habermann, D., and Richter, D.K., 1995, Kathodolumineszenz: Methodik und Anwendung. Zentralblatt für Geologie und Paläontologie Teil I, H ½, p. 287–306.

Oakes, C.S., Bodnar, R.J., and Simonson, J.M., 1990, The system NaCl-CaCl2-H2O. I. The ice liquidus at 1 atm total pressure: Geochimica et Cosmochimica Acta, v. 54, p. 603-610.

Steele-MacInnis, M., Lecumberri-Sanchez, P., and Bodnar, R.J., 2012, HOKIEFLINCS-H_2O-NACL: A Microsoft Excel spreadsheet for interpreting microthermometric data from fluid inclusions based on the PVTX properties of H_2O–NaCl, Computational Geosciences, v. 49, p. 334–337.

TABLE DR1: SAMPLE LOCATIONS AT THE WOLVERINE DEPOSIT

Sample name/ Company drill hole name	Long (WGS84)	Lat (WGS84)	Core depth (m)
BRWT-0228.3	128.940211	-18.85813	258.00–258.21
BRWT-0241.6	128.939728	-18.858039	240.60–240.64
BRWT-0268.4	128.93895	-18.857415	328.54–328.67
BRWT-0324.6	128.938684	-18.85709	419.31–419.44
BRWT-0324.1	128.938684	-18.85709	361.47–361.62

TABLE DR2: MICROTHERMOMETRIC DATA OF PRIMARY FLUID INCLUSIONS IN QUARTZ

Sample	FIA	No. of FIs	Quartz generation	Phases at T_{lab}	Occurrence	T_m(ice) range (°C)	T_h(LV→L) range (°C)	Salinity range* (wt.% $NaCl_{eq}$)
BRWT-0324.1	1	7	1	L-V	Cluster	-0.5 to -0.9	160 – 170	0.9 – 1.6
	2	5	1	L-V	Cluster	-1.2 to -0.6	150 – 165	1.1 – 2.1
	3	9	2	L-V-(S) **	Growth zone***	-25.2 to -24	107 – 100	25 – 25.7
	4	8	2	L-V-(S) **	Growth zone***	-24.7 to -23	115 – 103	24.3 – 25.4
BRWT-0228.3	5	7	2	L-V	Growth zone***	-24 to -21	115 – 110	23 – 25
BRWT-0241.6	8	4	2	L-V	Growth zone***	-25.4 to -23.8	120 – 118	22.9 – 25.8
BRWT-0268.4	9	3	2	L-V	Growth zone***	-23.3 to -22.5	115 – 114	24 – 24.5
BRWT-0324.6	6	4	3	L-V	Growth zone	-14.4 to -11.5	86 – 75	15.5 – 18.1
	7	4	3	L-V	Growth zone	-14.7 to -10.8	95 – 90	14.8 – 18.4

Note: FIA=Fluid inclusion assemblage, L: Liquid, V: Vapor, S: Solid.

*Calculated with HOKIEFLINCS, Steele-MacInnis et al. (2012).

**Some inclusions within the assemblage contain solid phases trapped accidentally (i.e. not daughter phases). Identified by laser Raman spectroscopy as anhydrite and hematite.

***Heterogeneously trapped inclusions with variable liquid:vapor volumetric ratios. Only inclusions rich in liquid have been analysed (see text).

TABLE DR3: LA-ICP-MS ANALYSES OF MAJOR AND SELECTED TRACE ELEMENTS IN INDIVIDUAL FLUID INCLUSIONS IN QUARTZ-2 NORMALIZED TO Na (g/g_{Na})

Sample	FIA	Inclu-sion No.	Na	Mg	K	Ca	Fe	Cu	Zn	Y	Pb	U
BRWT-0324.1	FIA 3	1	1	0.1860	1.2644	0.3154	0.2287	0.0162	0.0561	0.0045	0.0017	0.00008
		2	1	1.7693	2.4659	0.4953	0.0844	0.0226	0.0229	0.0001	0.0021	0.00003
		3	1	0.7073	1.3411	0.2102	0.3305	0.0203	0.0320	0.0002	0.0010	0.00006
		4	1	0.2374	3.1809	0.1866	0.5220	0.0244	0.0106	0.0002	0.0012	0.00001
		5	1	0.2761	0.9162	0.2153	0.1522	0.0111	0.0128	0.0001	0.0015	0.00039
		6	1	1.0470	1.6671	0.4338	0.3691	0.0250	0.0174	0.0002	0.0091	0.00060
		7	1	0.5436	2.7768	0.2034	0.0552	0.0328	0.0187	0.0002	0.0019	0.00003
		8	1	1.9933	1.5269	0.3195	0.0991	0.0287	0.0149	0.0004	0.0022	0.00005
		9	1	0.7153	1.1114	0.2787	0.1924	0.0703	0.0157	0.0002	0.0074	0.00034
BRWT-0324.1	FIA 4	1	1	0.2732	1.4238	0.1397	0.0595	0.0165	0.0079	0.0012	0.0013	0.00002
		2	1	0.3373	1.1652	0.2564	0.1489	0.0102	0.0058	0.0022	0.0015	0.00001
		3	1	0.2706	1.1872	0.3149	0.1064	0.0147	0.0099	0.0012	0.0020	0.00002
		4	1	0.5147	1.9580	0.2888	0.0544	0.0060	0.0050	0.0028	0.0027	0.00002
		5	1	0.3227	0.6552	0.1731	0.0574	0.0015	0.0063	0.0012	0.0017	0.00002
		6	1	0.5896	2.2923	0.4411	0.0997	0.0149	0.0062	0.0081	0.0027	0.00027
		7	1	0.4668	1.8531	0.2960	0.0755	0.0109	0.0072	0.0404	0.0016	0.00277
		8	1	0.7508	1.4262	0.2796	0.0732	0.0156	0.0075	0.0173	0.0023	0.00173
BRWT-0228.3	FIA 5	1	1	0.2399	1.4582	0.3930	0.1525	0.0155	0.0115	0.0005	0.0034	0.00004
		2	1	1.2129	2.7635	0.2887	0.0505	0.0160	0.0188	0.0001	0.0016	0.00007
		3	1	0.2566	1.0243	0.3938	0.1928	0.0181	0.0273	0.0004	0.0016	0.00016
		4	1	1.5785	0.9866	0.1286	0.2246	0.0108	0.0141	0.0004	0.0010	0.00001
		5	1	0.8653	3.0883	0.5262	0.2034	0.0166	0.0495	0.0030	0.0078	0.00076
		6	1	0.4429	2.2646	0.2826	0.1268	0.0168	0.0065	0.0031	0.0017	0.00013
		7	1	0.3394	1.0950	0.3983	0.1009	0.0487	0.0313	0.0008	0.0049	0.00002

Note: FIA=Fluid inclusion assemblage.

TABLE DR4: LA-ICP-MS ANALYSES OF TRACE ELEMENTS IN INDIVIDUAL FLUID INCLUSIONS IN QUARTZ-2 NORMALIZED TO Na (g/g_{Na})

Sample	FIA	Inclu-sion No.	Na	La	Ce	Pr	Nd	Sm	Eu	Gd	Tb	Dy	Ho	Er	Tm	Yb	Lu
BRWT-0324.1	FIA 3	10	1	0.00023	0.00016	0.00011	0.00062	0.00072	0.00019	0.00066	0.00010	0.00040	0.00010	0.00034	0.00009	0.00042	0.00009
		11	1	0.00007	0.00007	0.00005	0.00026	0.00030	0.00008	0.00028	0.00004	0.00020	0.00004	0.00015	0.00004	0.00047	0.00006
		12	1	0.00014	0.00020	0.00021	0.00053	0.00061	0.00016	0.00057	0.00008	0.00075	0.00012	0.00025	0.00008	0.00036	0.00011
		13	1	0.00023	0.00022	0.00030	0.00086	0.00013	0.00026	0.00092	0.00013	0.00055	0.00013	0.00040	0.00013	0.00059	0.00013
		14	1	0.00009	0.00011	0.00012	0.00034	0.00054	0.00010	0.00036	0.00005	0.00021	0.00005	0.00016	0.00005	0.00023	0.00005
		15	1	0.00020	0.00061	0.00015	0.00040	0.00046	0.00012	0.00043	0.00006	0.00042	0.00010	0.00027	0.00006	0.00027	0.00006
		16	1	0.00028	0.00019	0.00013	0.00075	0.00086	0.00022	0.00079	0.00011	0.00048	0.00012	0.00035	0.00011	0.00051	0.00011
		17	1	0.00043	0.00071	0.00013	0.00056	0.00025	0.00002	0.00030	0.00001	0.00011	0.00012	0.00006	0.00002	0.00005	0.00002
		18	1	0.00010	0.00006	0.00004	0.00022	0.00026	0.00007	0.00024	0.00003	0.00014	0.00005	0.00010	0.00003	0.00015	0.00003
BRWT-0324.1	FIA 4	9	1	0.00004	0.00006	0.00002	0.00012	0.00014	0.00006	0.00018	0.00002	0.00008	0.00003	0.00008	0.00003	0.00016	0.00002
		10	1	0.00009	0.00024	0.00002	0.00005	0.00006	0.00003	0.00014	0.00002	0.00009	0.00007	0.00003	0.00001	0.00007	0.00001
		11	1	0.00105	0.00054	0.00004	0.00025	0.00028	0.00013	0.00037	0.00004	0.00016	0.00007	0.00016	0.00005	0.00033	0.00005
		12	1	0.00200	0.00008	0.00003	0.00002	0.00002	0.00001	0.00007	0.00004	0.00027	0.00001	0.00021	0.00002	0.00031	0.00003
		13	1	0.00010	0.00007	0.00054	0.00027	0.00031	0.00014	0.00041	0.00004	0.00017	0.00007	0.00018	0.00004	0.00037	0.00004
		14	1	0.00043	0.00007	0.00001	0.00008	0.00009	0.00004	0.00011	0.00002	0.00021	0.00003	0.00007	0.00001	0.00022	0.00001
		15	1	0.00002	0.00010	0.00000	0.00002	0.00002	0.00001	0.00002	0.00000	0.00001	0.00000	0.00009	0.00000	0.00002	0.00000
		16	1	0.00003	0.00004	0.00002	0.00025	0.00013	0.00006	0.00050	0.00010	0.00007	0.00014	0.00049	0.00007	0.00053	0.00010
BRWT-0228.3	FIA 5	8	1	0.00026	0.00014	0.00010	0.00057	0.00065	0.00017	0.00060	0.00009	0.00036	0.00009	0.00055	0.00008	0.00039	0.00009
		9	1	0.00016	0.00020	0.00020	0.00060	0.00069	0.00018	0.00063	0.00009	0.00075	0.00012	0.00028	0.00009	0.00041	0.00009
		10	1	0.00005	0.00014	0.00006	0.00018	0.00029	0.00005	0.00019	0.00003	0.00011	0.00003	0.00008	0.00003	0.00012	0.00003
		11	1	0.00007	0.00021	0.00002	0.00013	0.00015	0.00004	0.00014	0.00002	0.00008	0.00002	0.00006	0.00002	0.00009	0.00002
		12	1	0.00020	0.00019	0.00027	0.00076	0.00050	0.00023	0.00081	0.00012	0.00049	0.00012	0.00035	0.00011	0.00052	0.00012
		13	1	0.00010	0.00012	0.00013	0.00037	0.00059	0.00011	0.00039	0.00006	0.00023	0.00006	0.00017	0.00005	0.00025	0.00006
		14	1	0.00021	0.00061	0.00015	0.00039	0.00036	0.00009	0.00033	0.00005	0.00042	0.00009	0.00028	0.00006	0.00021	0.00006

Note: FIA=Fluid inclusion assemblage.

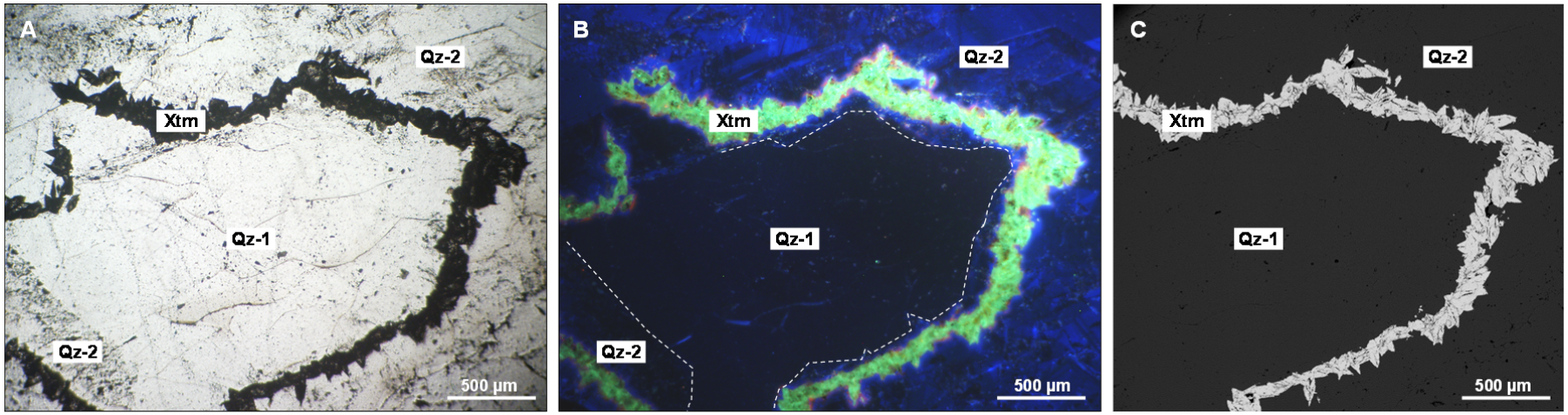

Figure DR1: (A) Transmitted light image, (B) CL image and (C) BSE image of euhedral xenotime crystals mantling quartz-1. The contrast of image (C) has been chosen to show details of xenotime, leaving quartz black.

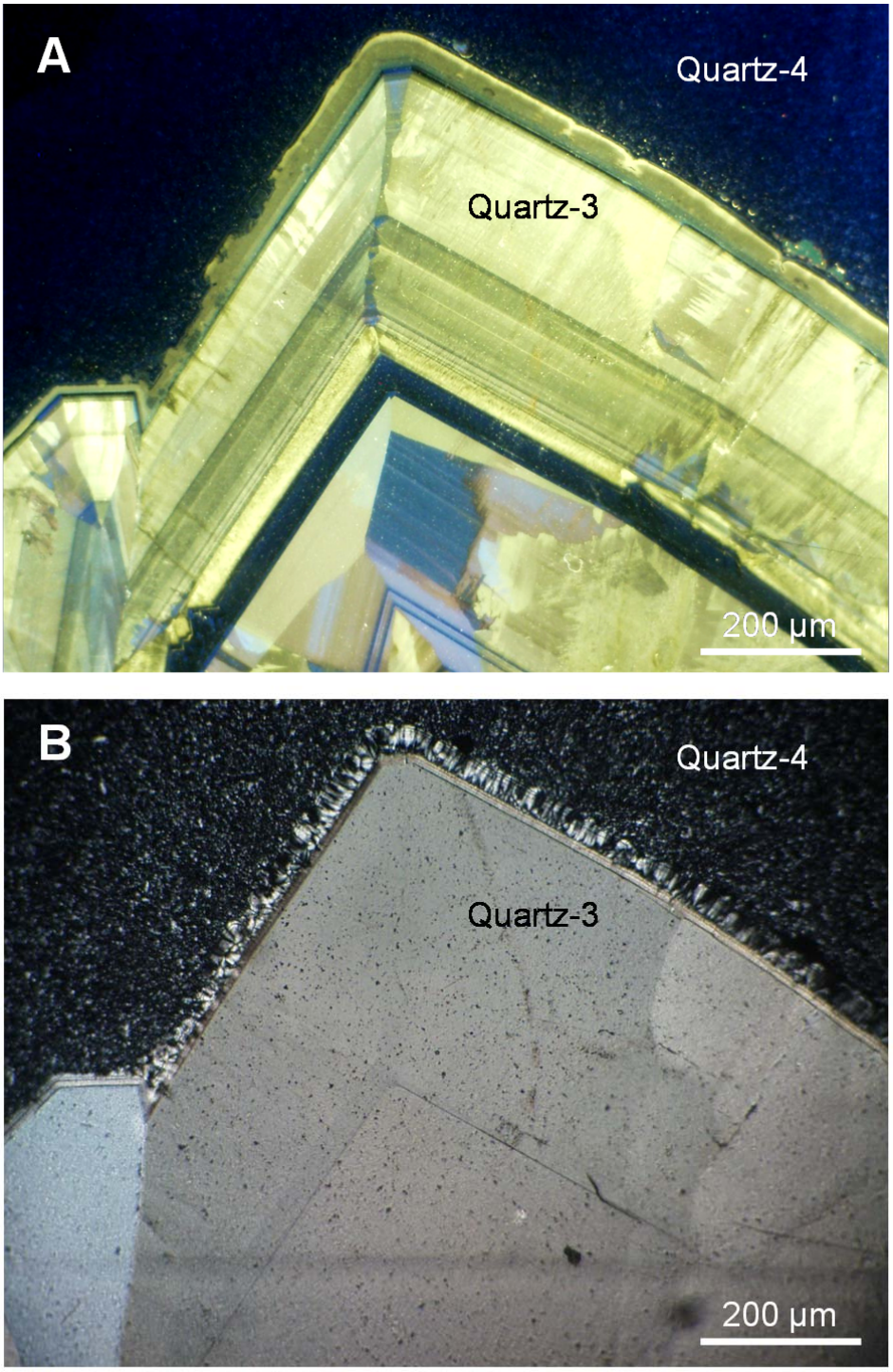

Figure DR2: (A) Cathodoluminescence (CL) image (top) and (B) cross-polarized light (bottom) microphotographs of quartz-3 (yellow in CL) and overgrowing quartz-4 (fine-crystalline, dark blue in CL).

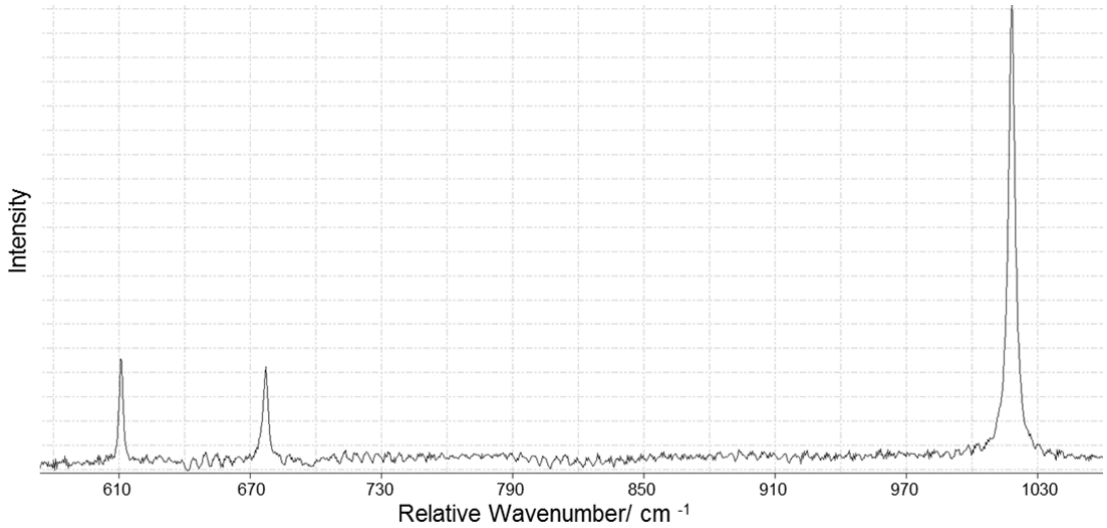

Figure DR3: Laser Raman spectrum of accidentally trapped anhydrite as a solid phase in primary fluid inclusions in quartz-2.

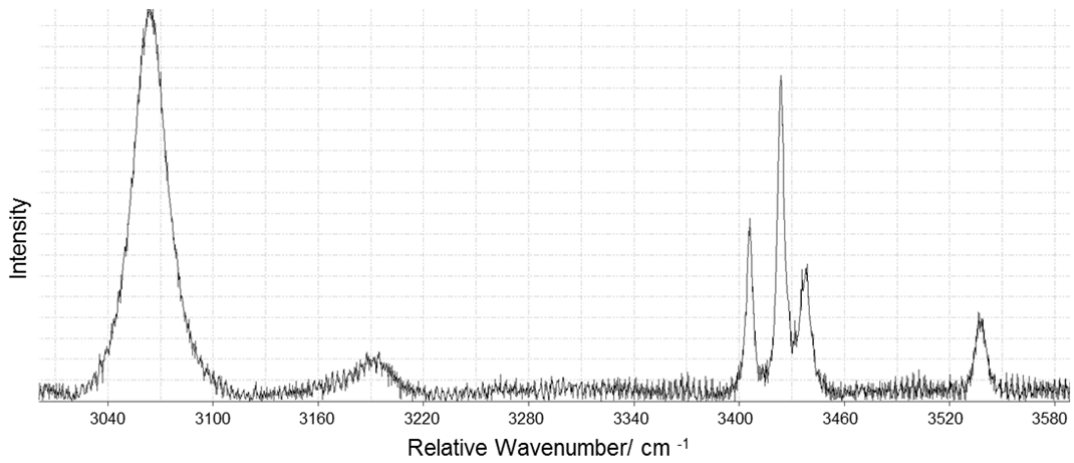

Figure DR4: Laser Raman spectrum of hydrohalite ($NaCl{\cdot}2H_2O$) in primary fluid inclusions in quartz-2, measured below the eutectic temperature at -190 °C.

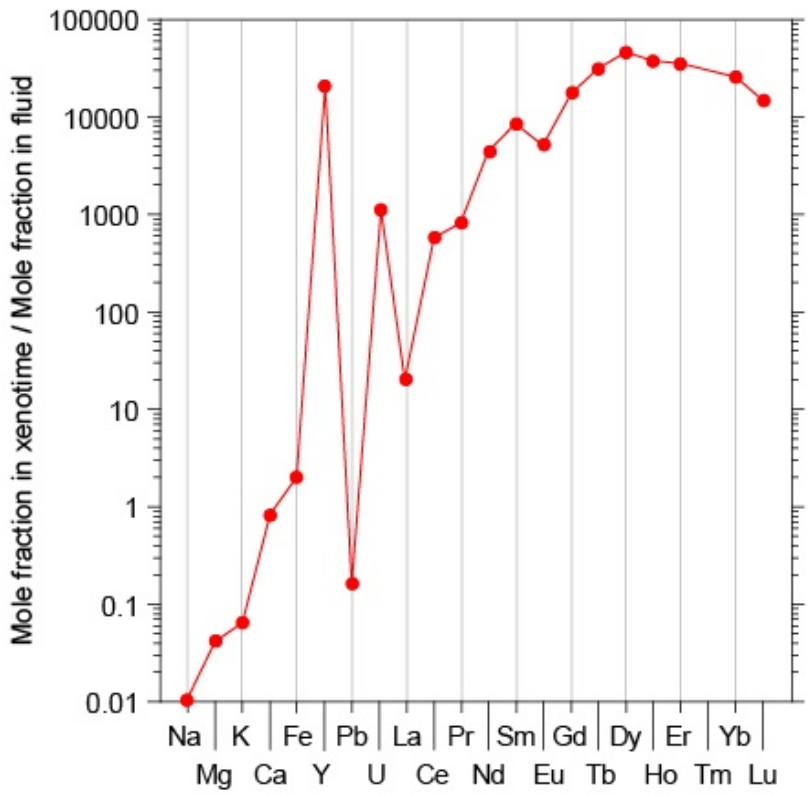

Figure DR5: Partition coefficients of analyzed elements between xenotime and its parent hydrothermal fluid at 100 °C and 1–2 bar.

TABLE DR5: MEAN ELEMENT MOLE FRACTIONS AND PARTITION COEFFICIENTS BETWEEN XENOTIME AND ITS PARENT HYDROTHERMAL FLUID AT 100 °C AND 1-2 BAR.

Element	Mole fraction in xenotime*	Mole fraction in parent fluid of xenotime	Molality (mol/kg_{H2O}) in parent fluid of xenotime	(Mole fraction in xenotime) / (mole fraction in fluid)
Na	1.88E-04	1.82E-02	1.17E+00	1.03E-02
Mg	4.87E-04	1.15E-02	7.36E-01	4.25E-02
K	1.21E-03	1.83E-02	1.17E+00	6.64E-02
Ca	2.65E-03	3.16E-03	2.03E-01	8.38E-01
Fe	2.40E-03	1.18E-03	7.55E-02	2.04E+00
Cu		1.33E-04	8.55E-03	
Zn		1.11E-04	7.14E-03	
Y	3.70E-01	1.75E-05	1.12E-03	2.12E+04
Pb	9.20E-07	5.56E-06	3.57E-04	1.66E-01
U	6.30E-04	5.61E-07	3.60E-05	1.12E+03
La	1.73E-05	8.34E-07	5.35E-05	2.08E+01
Ce	3.84E-04	6.41E-07	4.12E-05	5.99E+02
Pr	3.01E-04	3.53E-07	2.27E-05	8.52E+02
Nd	4.58E-03	1.04E-06	6.69E-05	4.39E+03
Sm	8.50E-03	9.77E-07	6.28E-05	8.70E+03
Eu	1.58E-03	2.96E-07	1.90E-05	5.34E+03
Gd	1.90E-02	1.05E-06	6.74E-05	1.81E+04
Tb	4.66E-03	1.48E-07	9.53E-06	3.14E+04
Dy	3.40E-02	7.27E-07	4.67E-05	4.68E+04
Ho	7.17E-03	1.89E-07	1.21E-05	3.80E+04
Er	1.90E-02	5.39E-07	3.46E-05	3.53E+04
Tm		1.32E-07	8.50E-06	
Yb	1.86E-02	7.12E-07	4.57E-05	2.61E+04
Lu	4.81E-03	3.24E-07	2.08E-05	1.48E+04

* Average of 86 spot analyses of xenotime by LA-ICP-MS from Cook et al. (2013)